Lasers in Manufacturing and Materials Processing (2024) 11:469–491
https://doi.org/10.1007/s40516-024-00256-7

RESEARCH

Influence of Polymer Surface Roughness on the Fractions of Transmitted, Reflected and Absorbed Energy in Operation of Laser Transmission Welding

Silvio Genna[1] · Claudio Leone[2] · Patrizia Moretti[1] · Simone Venettacci[3]

Accepted: 18 April 2024 / Published online: 30 April 2024

Abstract

The study of energy fractions plays a fundamental role in laser joining operations: from their knowledge, it is possible to calculate the amount of laser beam energy that is effectively available during the formation of chemical and physical bonds, and how much energy is dissipated. This study examines semi-crystalline polymers of polyamide 6.6 (PA), polyethylene terephthalate (PET), polytetrafluoroethylene (PTFE), and polypropylene (PP), semitransparent to light radiation, with the aim of studying the influence of surface roughness on the distribution of energy fractions, and in particular on the reflection portion. For this purpose, polymeric samples with different surface finishing were prepared and characterized by profilometric analysis. Subsequently, an experimental setup was implemented to directly measure the transmitted ratio, obtaining the reflected energy fraction from the Beer-Lambert law, and the absorbed ratio by energy balance. The results showed a decrease in the power transmitted by polymers subjected to surface treatment, due to an increase in the reflection fraction, a phenomenon particularly evident for PET, for which the reflection share increased from ~0.5% to ~15.3%, following P240 treatment. A lower influence was verified for PA and especially PTFE, due to a lower influence of the treatment on surface morphology. On the basis of the experimental results, it is hypothesised that roughening the lower section of the irradiated polymer could allow an increase in the total internal reflection fraction, favouring the joint at the interface point.

Keywords Laser transmission welding · Diode laser · Polymer · Surface finishing · Energy fractions · Beer-Lambert law

Extended author information available on the last page of the article

Introduction

The widespread use of plastics in the advanced technological field and day-to-day life requires a welding process that is fast, flexible, and environment friendly [1–3]. As a new approach to satisfying these demands, laser welding of plastics evolved in the last quarter of the 20th century [3–7]. Laser welding is receiving the highest attention in laser materials processing [8, 9]. Over the years, the laser welding technique gradually replaced plastic welding techniques which are based on friction, vibration, ultrasonic energy, electrical resistance, etc. in many applications. The advantages of innovative systems based on laser technology concern the elimination of mechanical fastening elements, solvents and adhesives in the joints, as well as the possibility of increasing the level of production automation [3, 10–14]. The use of a laser-based process shows advantages due to the possibility of the beam shaping, and, therefore, to an adjustable temperature-time profile for the joining process and to a locally limited energy input [15].

Laser transmission welding (LTW) of polymers has become an independent segment of laser technology and has significant scientific and industrial potential [16], thanks to superior weld quality and mechanical performance over conventional processes [17, 18]. In addition, a significant variation of this technique is represented by the laser joining technology of polymer-metal hybrid structures, which allows the production of new generations of joint solutions [19]. Laser welding is one of the most promising joining techniques to realize hybrid joints between metals and polymers [20]. LTW involves the transmission and absorption of radiation in polymers, heat generation, heat diffusion, melting, fusing, and re-solidification. The operation principle of the LTW involves the assembly of two elements with different optical properties, one of which must be laser beam-transparent or translucent and the other must be laser radiation-absorbing (opaque) [21]. In the case of polymer-metal hybrid joints, it is the metal element that represents the laser light-absorbing part [22].

These processes are achieved through the application of heating and compression pressure at the joint interface. As the laser radiation passes through the transparent polymer and incidents on the opaque metal surface, at the interface of the joint, part of the absorbed optical energy is transferred back towards the polymer by conduction, thus causing the melting of a thin layer which in turn spreads and coalescences with the metal surface due to the applied pressure. This causes a transformation in the state of the polymer-metal hybrid structures. During this process, a crystal structure can be reorganized and the polymer may reach its melting temperature to form a hybrid joint [8]. This technology represents a fast, flexible, and non-contaminating welding process for producing aesthetic and high-quality polymer joints [2, 18, 23]. However, when a laser beam with narrow gaussian distribution is adopted, a localized heat-affected zone may be produced, inducing low thermal and mechanical stresses during LTW [14].

In this context, a variety of pre-treatment methods for metal substrates or polymers can improve the bonding strength. The low chemical affinity between different materials can partly be overcome by roughing the metal surface. During the laser joining, the polymeric material reaches such a high temperature and low viscosity

to flow inside the obtained grooves. This method allows significantly enhances the bonding between the metal and the polymer-based materials through the formation of micromechanical interlocking at the joint. Currently, many pre-treatment methods target metal substrates prior to the laser joining process, while pre-treatment of polymer substrates is rare and can be subject to further investigations [15].

Key aspects of the described joining method refer to the brevity of the laser beam-polymer interaction time, as well as to the fact that only a part of the laser radiation striking the polymer surface is reflected, and an even lower part reaches the joint point. Therefore, optimal process conditions should require a surplus of energy with respect to the theoretical one required for fusion. In semi-crystalline polymers (such as those considered in this research) the absorbed amount is attenuated as the radiation crosses the polymer, and the attenuation is a function of the path length. The crystalline structure increases the light travel path, thereby increasing the probability of either being absorbed or backscattered [14]. This light scattering occurs spontaneously in the polymer by single or multiple reflections and refractions [11, 24]. The presence of various phases, such as amorphous, crystalline, or even additives (typically used to impart colouration) o reinforcing (such as glass fibres), increases the level of interactions among laser beam and phase boundaries, producing substantially more scattering [9, 11]. Due to enhanced backscattering in semi-crystalline polymers, apparent reflection increases with crystallinity and radiation dispersion is greater than in amorphous ones. For instance, compared to PA6, PA66 was found less transmittable since its higher level of crystallinity [14, 23].

The surface quality, as well as the crystallinity and the part thickness also affect the optical properties of polymers and LTW process outputs [14]. The light reflection and scattering are found to be extremely dependent on the sample surface finish. As a result, surface morphology is an important factor that influences the distribution of energy fractions in the LTW process.

The surface finish is not only important for the visual appearance of the structure, but is also related to durability, affecting the adhesion and interlocking between layers.

The morphology and the roughness of the surface are among the main factors that affect laser transmission welding processes, as they influence the absorption of the material. In laser joining, a metallic material with a smooth surface shows only less than ten per cent of radiation absorption; moreover, the absorption of polymeric materials is affected by the angle of incidence of the laser beam, which is in turn related to the material surface roughness. For metallic and non-metallic materials, different methods can be used to improve absorption; among these, the control and improvement of the surface morphology represent a very effective solution [25].

Therefore, an investigation of the relationship between absorbing material and surface roughness turns out to be significant. Su et al. [26] found that different types of surface morphology have different effects on the capacity and modality of reflection and significantly influence the absorption of materials. They analysed the ability to increase absorbance and angle of incidence characteristics of light, creating different surface morphology. Chen et al. [27] established a computational model to describe the influence of surface roughness on laser beam

absorption. Wang et al. [28] observed that the scattering of a PP plaque increases with the surface roughness.

Some authors created a solution allowing simultaneous measurement of the light transmission and reflection of clear rigid polyvinyl chloride (PVC) from a diode laser source. The quantity and distribution of light reflection were found to be dependent on the surface finish: 8% and 16% of the incident laser beam is reflected from samples with the smoothest and roughest surface finish, respectively. Furthermore, the light is reflected in a specular way by the smooth samples, while it is much more diffused by the sand-blasted samples [29].

The cited studies highlight the influence of surface finish in the operations of hybrid metal-polymer laser joints. In general, researchers have shown that the surface finish of the metal directly influences the efficiency and tightness of the joint, ensured through an interlocking mechanism. The surface finish of the polymeric part instead mainly concerns the influence of the roughness on the distribution of the laser light beams. Surface roughness is in fact closely linked to the ability to absorb radiation, which in semi-crystalline polymers can penetrate to a thickness of a few millimetres, unlike non-pigmented amorphous plastics, where it penetrates along the entire thickness. While the reflected fraction is influenced by the surface roughness, the transmitted energy share is influenced by the degree of crystallinity of the polymer and by the possible presence of additives. Therefore, for transparent semi-crystalline polymers, the study of the energy fractions is of fundamental importance for the realization of an effective joint. Some authors report that for semi-crystalline polymers laser transmission is dependent on part thickness which has an impact on optical properties. Conversely, part thickness is not a major concern for laser transmission in amorphous polymers, which are non-crystalline [10, 11]. The latter affects the absorbed and scattered energies, then the laser beam intensity decreases monotonically with an increase in polymer part thickness [14]. The transmissivity of natural PA6 decreases from 81% to 70% hen inceasing the part thickness from 1 mm to 3 mm [10]. The transmissivity of PA6, PE (Polyethylene) and PP, in their natural state, are observed to be reduced from 85.3%, 80.9% and 7.1%, espectivel to 20.4%, 12.1% and 0.4% byincreasin the part thickness from 1 mm to 10 mm [22, 30].

The distribution of energy fractions associated with a laser beam passing through a polymer can be determined using the attenuation's law (i.e., Beer-Lambert law), which describes the attenuation of light intensity within a material as the thickness varies (please refer to the characterization procedure of "Materials and Characterization Procedure" section). S. Genna et al. in [31] characterized the laser beam transmission through a High-Density Polyethylene (HDPE) plate. The authors measured the transmitted power with a power meter and the reflected power by applying the Beer-Lambert law to samples of different thicknesses. The absorbed ratio was measured by infrared (IR) thermal images and the scattered ratio was obtained by energy balance.

The aim of this paper is to study the influence of surface roughness on the radiation energy shares distribution, in particular on the fraction of reflected radiation, with the aim of optimizing this parameter and ensuring the best joint efficiency. Since the surface roughness can cause radiation reflection in different angles, the

surface roughness may influence the amount of reflected radiation and the power of the incident radiation required to trigger the joining [32].

The behaviours of semi-crystalline polymers such as polyamide 6.6, polyethylene terephthalate, polytetrafluoroethylene, and polypropylene were investigated in this study. The experimental set-up was carried out with the aim of measuring the absorbed, transmitted and reflected energy fractions through the adoption of samples characterized by different roughness. The reflected energy percentage was measured by applying the Beer-Lambert law to samples with different thicknesses. The transmitted ratio was directly measured, while the absorbed ratio was measured by energy balancing as the difference between the incoming power and the other ratios. The scattered ratio has not been considered since it is not always present and is usually included in the absorbed light ratio.

In summary, this work aims to fill the gap in studies and knowledge on the influence of polymer surface roughness on the fractions of transmitted, reflected, and absorbed energy in LTW technology, a current subject of great industrial interest, due to its numerous possible applications in a wide range of industries, including automotive, medical devices, electronics, microtechnology, packaging and containers, textiles, etc., thanks to its competitive process advantages and cost-efficiency [17, 18, 21]. The goal of the study is therefore to obtain a good basis for producing reliable laser-assembled polymer-metal hybrid structure joints and to propose possible topics for future research.

Experimental

Sample Morphology

The roughness measurements on the PA, PET, PTFE, PP treated and AS (as-received) samples surface were carried by using the 3D Talysurf CLI 2000 surface profilometer (Taylor Hobson, Leicester, UK) equipped with an inductive stylus with a 2 µm radius movable tip, scanning the surface of the sample. The surface roughness was evaluated by recording 4 patterns, with an axial and vertical resolution of 0.5 µm and 8.28 nm, respectively. A sampling length of 20 mm was adopted. After acquisition, TalyMap R.3.1 software was adopted to get the main roughness parameters in accordance with the UNI EN ISO 4288:2000 standard. It represents the international reference standard for roughness measurement, accepted by the scientific community, guaranteeing correct reproducibility of measurements. More specifically, in order to characterize the surface topography, the arithmetic mean surface roughness (Ra) and the mean roughness depth (Rz) were calculated in height; the mean width of profile elements (RSm) was calculated horizontally.

Laser Equipment

The experimental tests were carried out by using a 200 W Diode laser (IPG DLR-200-AC) operating at a wavelength (λ) of 975 nm (near infrared). Diode

Table 1 Characteristics of the diode laser IPG-DRL-200-AC

Characteristics [Symbol]	Value	Unit
Emission centroid wavelength* [λc]	975 ± 5	[nm]
Emission linewidth* [Δλ]	6	[nm]
Nominal power (min) [P_n]	200	[W]
Modulation frequency	50	[kHz]
Output fibre core diameter	200	[μm]
Collimated output beam diameter **	6	[mm]
Beam parameter product [BPP]	22	[mm*mrad]
Cooling system	air	--
Power consumption***	600	[W]

*At P_n and Tcase = 25 °C

** At collimator exit

*** At the max power output

Table 2 Correspondence between set power and measured one with IPG DRL 200 laser source (with a beam wavelength of 975 nm)

Power set on display [%]	Measured power [W]
10	13.2 ± 0.5
20	39.9 ± 0.5
30	65.2 ± 0.5
40	90.5 ± 0.5
50	108.5 ± 0.5

laser sources are characterized by high energy efficiency (about 40%) and flat energy distribution, thus allowing a more homogeneous energy distribution, that represents an advantage in joining operations; during the polymer joining, a high focusing of the radiation is not required. The laser source is transferred via an optical fibre, 6 m in length, to a collimator resulting in a laser beam diameter of about 6 mm. The collimator was mounted on a 3 + 1 axis CNC machine (finecut Y 340 M, by Rofin). The computer controlled laser system allows the generation of the geometric patterns and the set-up of the process parameters, i.e., the laser beam power and the interaction time. Table 1 shows the detailed characteristics of the laser source. Since the power is regulated by means of the diode current setting, the laser source behaviour was characterized before the test by adopting a power meter (OPHIR F150A-SH sensor and Nova Display Assy by OPHIR). In Table 2 the experimentally measured laser beam power is reported as a function of the power set on display [%] (i.e., the percentage of the maximum diode current). This measurement is important to know the power of the laser radiation incident on the surface (P_L), which is present in Eqs. (1) and (3), reported in "Materials and Characterization Procedure" section.

Materials and Characterization Procedure

For each material (PET, PP, PTFE and PA) samples of 30×30 mm^2 were obtained by cutting from commercially available plates the as-received specimens. Polyethylene terephthalate (PET) plates were provided by NUDEC, S.A., while natural polypropylene (PP, code: 682 – 551), natural polyamide 6.6 (PA, code: 704–8144) and matt polytetrafluoroethylene (PTFE, code: 680 – 678) ones by RS Components S.r.l. The sample are reported in Fig. 1 and the thicknesses were 2.9 ± 0.1, 3.0 ± 0.1, 3.2 ± 0.1, 5.8 ± 0.1 mm for PET, PP, PTFE and PA, respectively. For the realization of different degrees of surface finish of the samples, abrasive papers of different grits were used (i.e., 180, 220, 240, 400, 600, 800 according to the classification of the European federation of abrasive paper producers, FEPA P). The higher the grit (i.e., the number of meshes in a sieve per square inch) the finer the abrasive. For the corrugation treatment of the specimens, a sanding machine with water was used, with a fixed processing time for all specimens. There was no progression in the use of papers, but only one paper per specimen was used. After the gritting procedure, the specimens were cleaned in an ultrasonic bath with isopropanol. Before performing the diode laser irradiation, roughness tests were carried out on the AS and abraded polymers. The power measurements for the different radiation shares were repeated three times for each thickness and for each type of treatment (AS, P180, P240, P400, P600, P800).

Figure 2 reports a schematic view of the set-up configuration used for the irradiation of samples with different degrees of surface finish. Samples cut from the original plates were placed below the laser beam. On the opposite face of the sample, just below the plate, the power sensor was placed and connected to the power meter. In this condition, the whole acquisition system accuracy is 75%. On

Fig. 1 Polymer samples treated with different abrasive papers and untreated ones

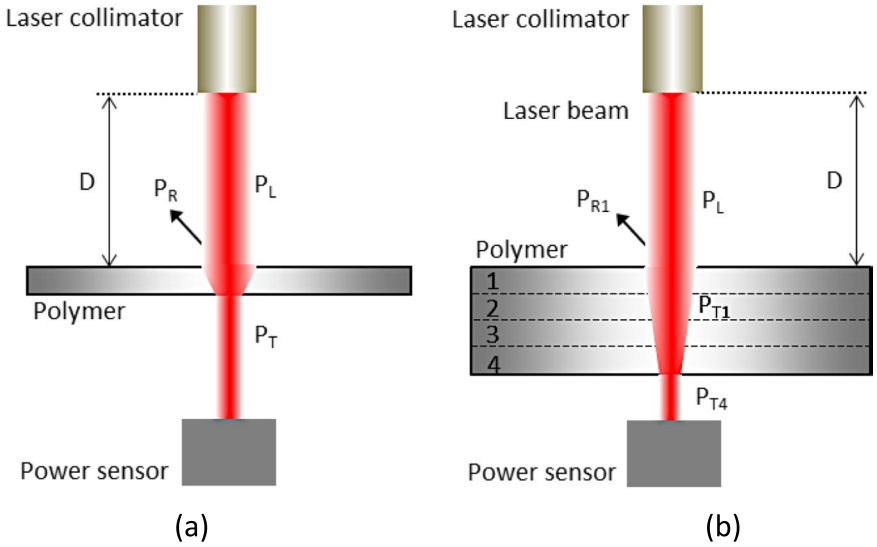

Fig. 2 Experimental set-up for the experimental determination of the Beer-Lambert law. PL, PR and PT are the incident, reflected and transmitted powers, respectively. **a** Single sample test; **b** multi-plate configuration

the opposite face of the plate, the diode laser collimator was placed. The power meter was manually reset before each measurement, and the average power was measured adopting a measuring time of 3 s, acquiring 3 measurements in the 10-second test period and calculating the average value. In order to test samples with different thicknesses, up to 4 samples were superimposed; to avoid reflection or scattering phenomena between the different samples, a clamping system was adopted. During the tests, the following parameters were fixed: working distance (D = 180 mm), which refers to the vertical distance between the laser collimator and the top surface of the polymeric plate; the treatment time (t = 10 s), i.e., the interaction time between laser beam and material. It is worth noting that since no focussing lens was present, directly taking the laser beam at the exit of the collimator, so the beam diameter does not change with the focussing distance, which is not important for experimental purposes. The treatment time was instead selected after preliminary tests, in order to avoid material degradation, which would affect the quality of polymer-metal hybrid joints [33], while also ensuring a good accuracy of measurement of the transmitted power, i.e., output from the plates, as measured by a power meter. Under these conditions, no damage of the exposed material was observed.

With reference to single sample test configuration of Fig. 2a, when laser light passes through the polymeric plate, a portion of the power of the laser radiation incident on the surface (P_L) is lost due to reflection at the surface (P_R), a portion is absorbed (P_A), another is transmitted (P_T). Thus, the energy balance equation can be written as:

$$P_L = P_T + P_R + P_A \quad (1)$$

In Eq. (1), P_L and P_T represent the terms that can be calculated with the experimental setup of Fig. 2a: P_L was directly measured by adopting the power meter without the polymer samples (i.e., the power sensor was directly irradiated by the laser radiation); P_T was measured by placing a polymeric material between the laser collimator and the power meter. This procedure was repeated for each material kind and treatment, taking care to position the faces with different roughness from the incoming side of the radiation (i.e., the upper surface).

According to [34], the distribution of radiation inside the polymer can be approximated by the Beer-Lambert law, which correlates the amount of radiation absorbed by the material to the thickness of the material itself. It can be approximated by an exponential law of the radiation against the thickness: when a beam of monochromatic light of intensity I_0 crosses a medium, part is absorbed by the medium itself and part is transmitted with residual intensity I, according to the Eq. (2):

$$I = I_0 e^{-kx} \quad (2)$$

where k is the attenuation coefficient.

The knowledge of this law, i.e., of the coefficients that regulate the absorption in the material, is of particular interest, as it allows to determine the transmitted energy fraction, as the thickness of the polymer varies.

By imposing $x = \varepsilon$ in the Beer-Lambert attenuation law, i.e., considering being an infinitesimal layer just inside the material, the power share that is present in the first layer of the material (P_0) can be calculated: this represents the power portion that effectively enters into the polymer. Consequently, the energy share lost on the surface by reflection (P_R) can be approximated as:

$$P_R = P_L - P_0 \quad (3)$$

Substituting all terms calculated and/or measured in the energy balance of Eq. (1), the energy share absorbed within the polymers can be calculated.

So far, for the materials following the Beer–Lambert law, equations can be easily calculated through regression analysis if samples with different thickness are available. Unfortunately, since the reflection index is a function of the surface roughness [35], the use of machined plate at different thickness is not recommended. A possible alternative is to use the "multi-layer" transmitted power measuring method [31], reported in Fig. 2b (multi-plate configuration test). This method assumes that, if two or more plates are cleaned and strongly superimposed to create a single sample, this sample behaves as a single plate with a thickness equal to the sum of the plate's thicknesses. This procedure was performed for a laser radiation power P_L of 100 W for PTFE and PA, of 50 W for PP and of 25 W for PET; such values were chosen to obtain a transmitted power of about 25 W, in the case of a single plate configuration. A number of plates up to 4, i.e., a thickness variable in the range of $\sim 3 \div 12$ mm for PET, PP and PTFE, and in the range of $\sim 6 \div 24$ mm for PET, was adopted as reported in Fig. 2b.

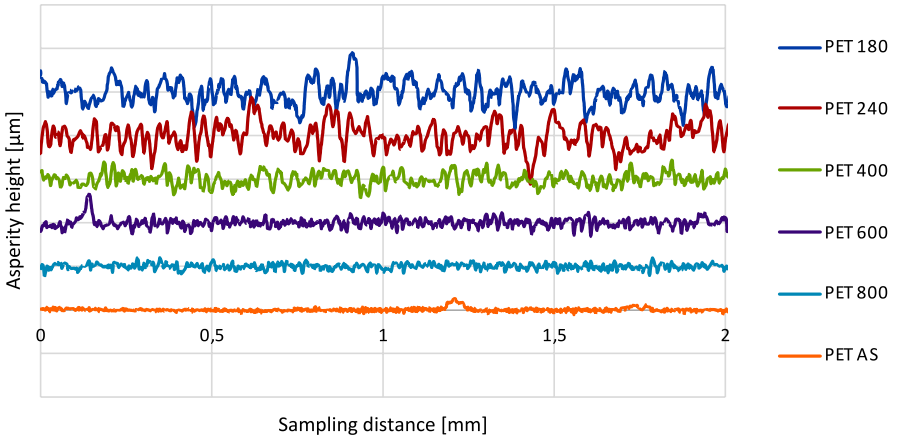

Fig. 3 Roughness profiles of PET samples treated with different abrasive papers. Please note that the height of each box is equal to 10 µm

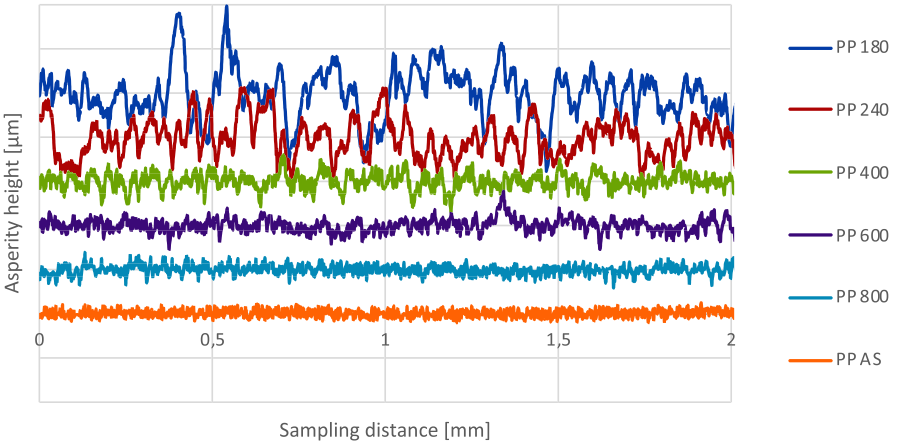

Fig. 4 Roughness profiles of PP samples treated with different abrasive papers. Please note that the height of each box is equal to 10 µm

Results and Discussion

Figures 3, 4, 5 and 6 show the first 2 mm of one of the ten profiles acquired by the profilometer for each material and treatment. It is worth noting how the smoothest surfaces correspond to the as-received sample (AS), while the treated surfaces are all the smoother the higher the grit of abrasive paper used in the treatment. Coarser grit papers, i.e., PA 180 and PA 240, wrinkle the material more, as they remove more material, thus removing it deeper. This is different with finer grit papers, which do not change the surface, which remains similar to the as-received specimen. Table 3 shows the measured roughness values for all the polymers examined.

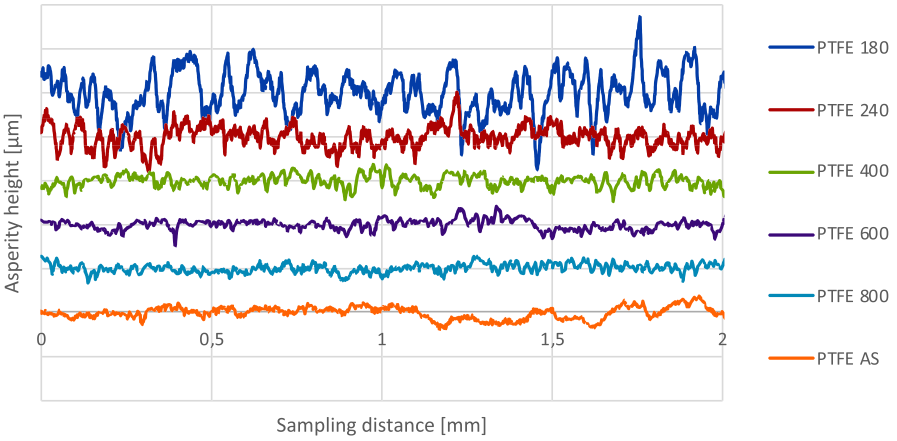

Fig. 5 Roughness profiles of PTFE samples treated with different abrasive papers. Please note that the height of each box is equal to 10 µm

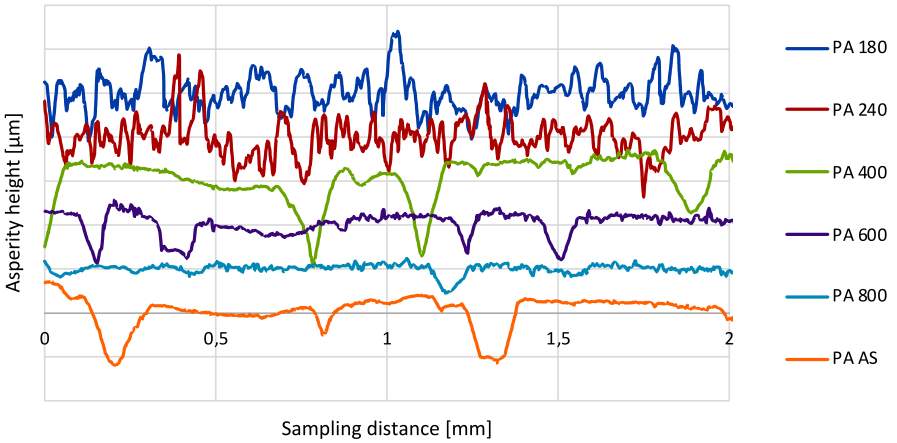

Fig. 6 Roughness profiles of PA samples treated with different abrasive papers. Please note that the height of each box is equal to 10 µm

The mean arithmetic height of the profiles (i.e., Ra) ranged from 0.037 to 2.328 µm for PET, from 0.140 to 2.980 µm for PP, from 0.428 to 2.180 µm for PTFE and from 0.300 to 3.906 µm for PA by processing with abrasive paper. The maximum height values of the roughness profiles (i.e., Rz) is significantly higher and increases by about 37, 13, 5, 6 times for PET, PP, PTFE, PA, respectively, following the abrasive treatment, ranging from 0.473 to 17.516 µm for PET, from 1.590 to 19.973 µm for PP, from 3.135 to 15.876 µm for PTFE and from 4.000 to 25.686 µm for PA.

Table 4 compares the response of the polymers examined following the final surface treatment with the lower grit abrasive (i.e., P180). PTFE suffers the least influence of surface treatment, since the as-received sample is associated with

Table 3 Roughness parameters for polymer samples treated with different abrasive papers

Polymer	Sandpaper	Ra [μm]	Rz [μm]	RSm [mm]
PET	AS	0.037	0.473	0.014
	800	0.244	2.177	0.021
	600	0.250	2.231	0.024
	400	0.698	5.800	0.032
	240	1.519	10.494	0.062
	180	2.328	17.516	0.055
PP	AS	0.140	1.590	0.029
	800	0.498	4.028	0.032
	600	0.626	5.125	0.036
	400	1.073	8.344	0.038
	240	2.400	17.565	0.057
	180	2.980	19.973	0.072
PTFE	AS	0.428	3.135	0.078
	800	0.457	3.122	0.073
	600	0.435	2.988	0.057
	400	0.578	3.846	0.068
	240	1.522	10.638	0.068
	180	2.180	15.876	0.066
PA	AS	0.300	4.000	0.357
	800	1.271	11.894	0.079
	600	1.060	8.442	0.032
	400	1.299	8.709	0.079
	240	2.812	18.256	0.075
	180	3.906	25.686	0.082

Table 4 Comparison between different materials: influence of surface treatment (with abrasive grit P180) on roughness parameters

Parameter	As-received (Interval range)	Post P180 treatment (Interval range)
Ra [μm]	PET < PP < PA < PTFE (~ 0.04 ÷ 0.43)	PTFE ≈ PET < PP < PA (~ 2.18 ÷ 3.91)
Rz [μm]	PET < PP < PTFE < PA (~ 0.47 ÷ 4.00)	PTFE ≈ PET < PP < PA (~ 15.88 ÷ 25.69)
RSm [mm]	PET < PP < PTFE < PA (~ 0.01 ÷ 0.36)	PET < PTFE ≈ PP < PA (~ 0.06 ÷ 0.08)

high values of the studied roughness parameters (i.e., Ra, Rz, RSm), highest for Ra and lower for Rz and RSm at PA alone, while post P180 treatment PTFE has the lowest values for Ra and Rz, reduced for RSm. PET maintains the lower values of the roughness parameters both before and after the treatment, showing that it is more affected by the surface treatment. Intermediate trends are shown by the PP and the PA, with the latter presenting the highest values of these parameters;

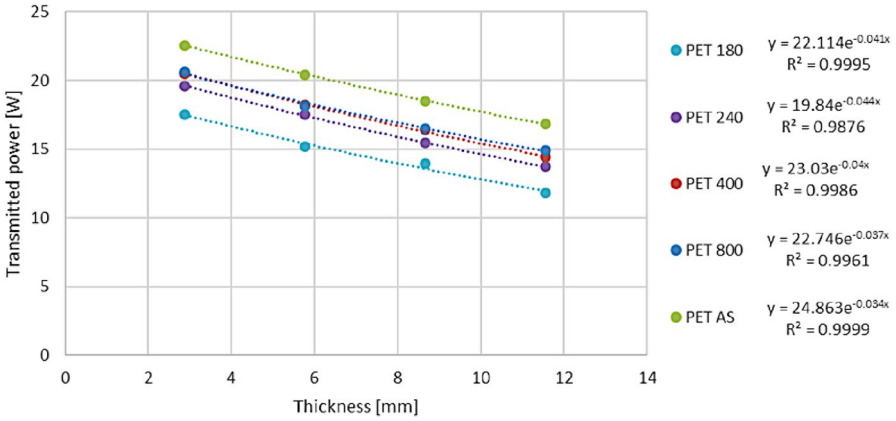

Fig. 7 PET: transmitted power as a function of the thickness and of the different surface finish (setting a P_L of 25 W)

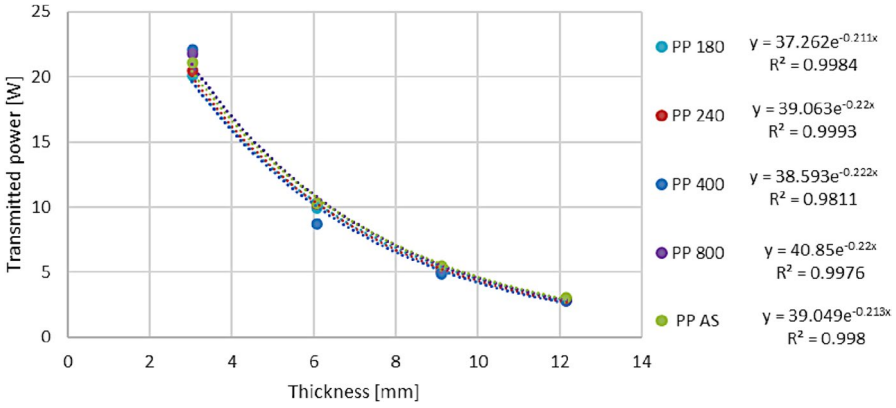

Fig. 8 PP: transmitted power as a function of the thickness and of the different surface finish (setting a P_L of 50 W)

after the PTFE, PA is the material that shows the minor influence of the abrasive treatment on the surface morphology.

The treated (abrasive treatments from P800 to P180) and untreated (AS) polymers were studied radiating the samples, according to the experimental set-up described in Fig. 2. Plotting the transmitted power (P_T) as a function of the thickness, it is possible to obtain the diagrams reported in Figs. 7, 8, 9 and 10, that represent the Beer-Lambert laws for the different polymeric plates exposed at a wavelength of 975 nm. All equations present in the graphs represent the best-fitting exponential equations of the experimental measures, while R^2 is the correlation factor between the exponential law and the experimental measures. It is worth noting that R^2 assumes values of ~ 1, for all the laser beam powers in consideration and materials, indicating that the experimental points fall very close to the exponential law. At these powers,

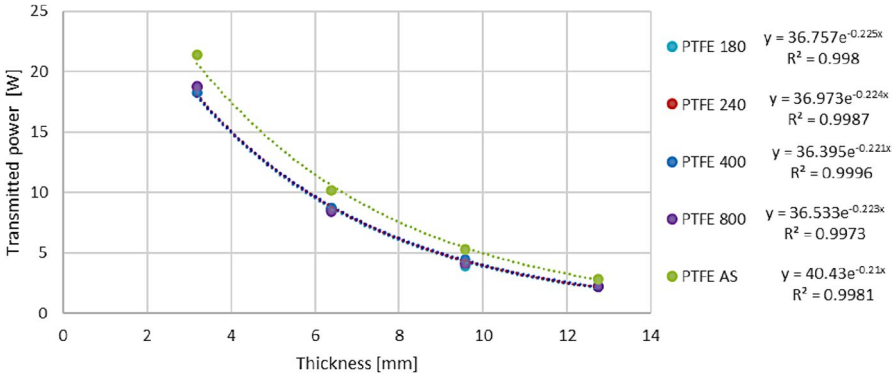

Fig. 9 PTFE: transmitted power as a function of the thickness and of the different surface finish (setting a P_L of 100 W)

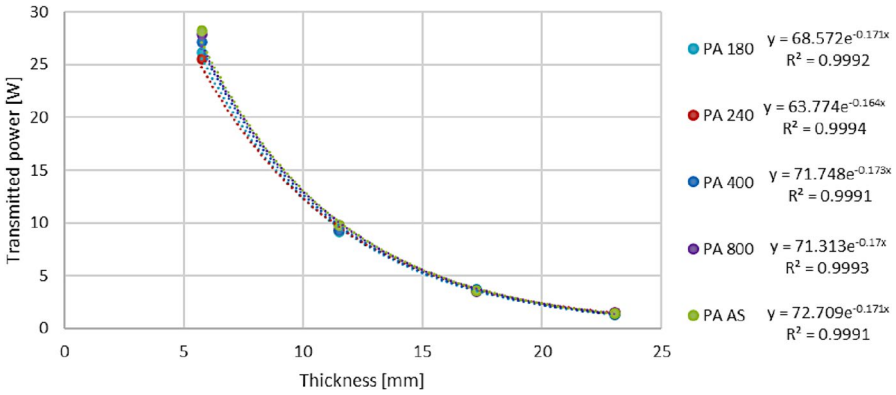

Fig. 10 PA: transmitted power as a function of the thickness and of the different surface finish (setting a P_L of 100 W)

as the surface finish varies, the maximum change in the exponential index that represents the "k" coefficient of Eq. (2), corresponds to about 29.4%, 4.2%, 7.1% and 4.1% for PET, PP, PTFE and PA, respectively, compared to AS samples.

The general trend of the graphs shows a maximum transmitted power for the AS samples and a decrease in the P_T of the polymers as the degree of surface roughness increases (i.e., as the grit of the sandpaper grows from P800 to P180), as well as increasing thickness (according to the attenuation effect reported in Eq. 2). In particular, an almost gradual decrease in the transmitted energy fraction is clearly visible in the case of PET (as reported in Fig. 7). For PTFE, the transmitted share decreases following the first treatment (i.e., P800) and then remains approximately constant (please refer to Fig. 9). For PP and PA, a minor influence of pre-treatment is instead observed, with very close and almost overlapping transmitted power curves (please refer respectively to Fig. 8 for PP and Fig. 10 for PA). The trends of the transmitted powers reflect well those of the roughness parameters previously

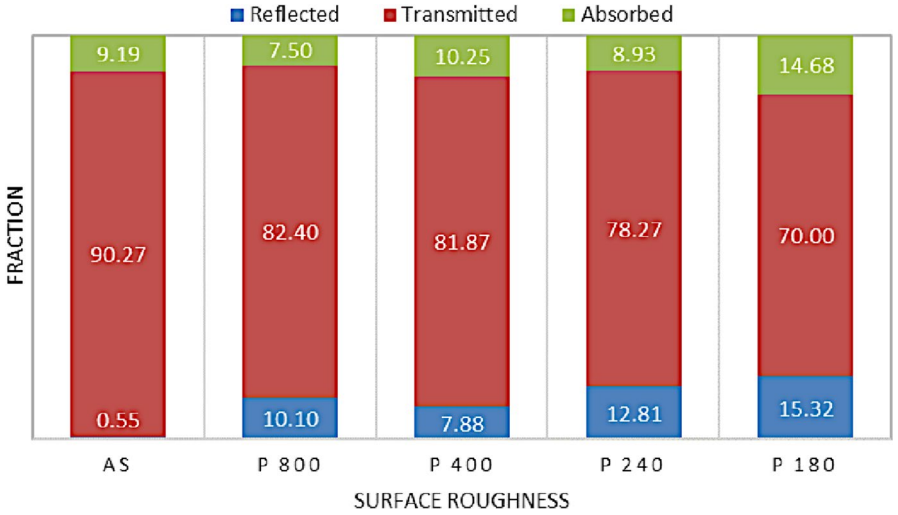

Fig. 11 PET: Percentages of reflected, absorbed, and transmitted energy fractions, at the wavelength $\lambda = 975$ nm, as a function of surface finish

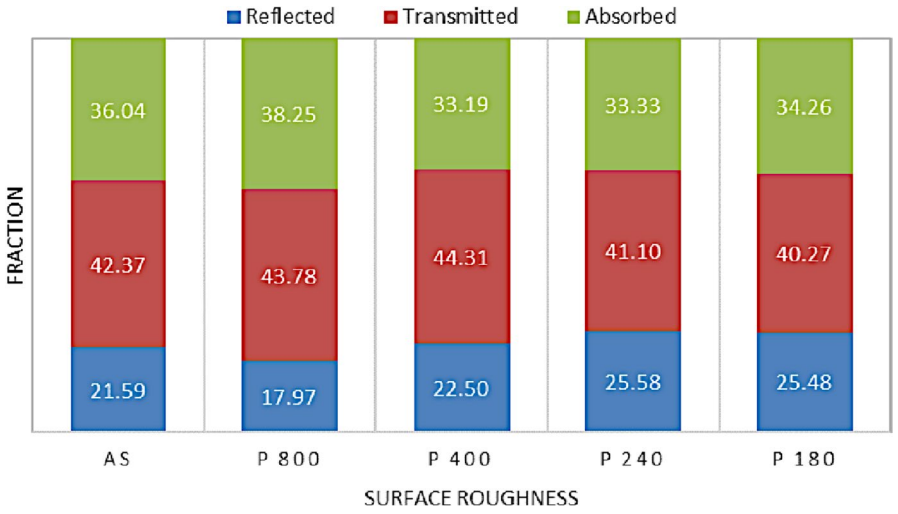

Fig. 12 PP: Percentages of reflected, absorbed, and transmitted energy fractions, at the wavelength $\lambda = 975$ nm, as a function of the surface finish

observed where the surface morphology of the PET showed the greatest dependence on the treatments applied (as reported in Fig. 3 and in Tables 3 and 4).

Plotting the percentages of absorbed, transmitted, and reflected energy of the different materials as a function of the surface finish in single-plate test configuration (refer to Fig. 2a), the histograms from Figs. 11, 12, 13 and 14 were obtained. The trends of the various energy fractions reflect the degree of opacity of the polymers

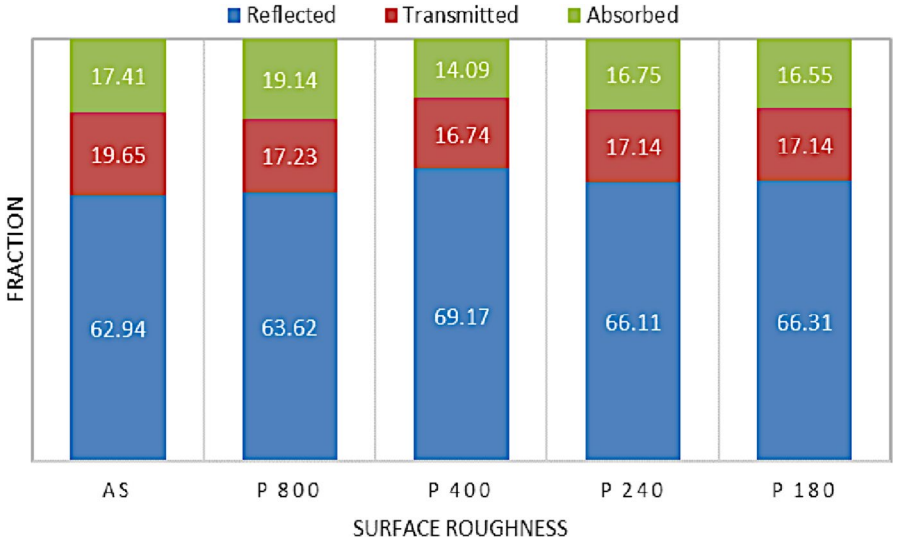

Fig. 13 PTFE: Percentages of reflected, absorbed, and transmitted energy fractions, at the wavelength $\lambda = 975$ nm, as a function of surface finish

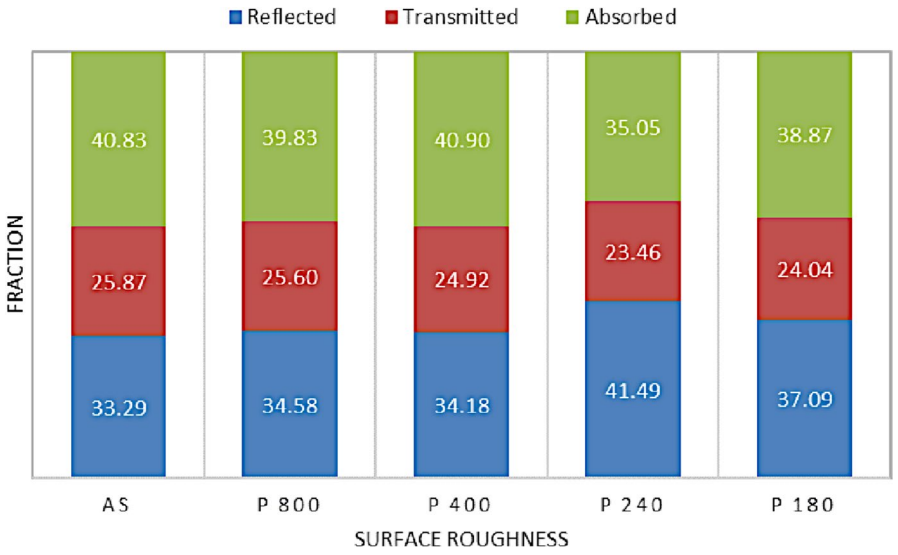

Fig. 14 PA: Percentages of reflected, absorbed, and transmitted energy fractions, at the wavelength $\lambda = 975$ nm, as a function of the surface finish

to the near-infrared radiation of the laser beam here investigated, which increases passing from PET (transparent) to PTFE (opaque), passing through the intermediate values of PA and PP. In fact, PET has the lowest percentages of absorbed and reflected energy fraction, both in the as-received sample and following treatments,

Table 5 Comparison of different materials: trend of the energy fractions distributions (RF, TF and AF) at the initial roughness and influence of surface treatment (P180)

Energy fractions distribution	Initial roughness (AS) (interval range)	Final roughness (P180) (interval range)
RF [%]	PTFE > PA > PP > PET (0.55 ÷ 62.94)	PTFE > PA > PP > PET (15.32 ÷ 66.31)
TF [%]	PET > PP > PA > PTFE (19.65 ÷ 90.27)	PET > PP > PA > PTFE (17.14 ÷ 70.00)
AF [%]	PA > PP > PTFE > PET (9.19 ÷ 40.83)	PA > PP > PTFE > PET (14.68 ÷ 38.87)

Table 6 Variation of the percentage distributions of the RF, TF and AF following surface treatments with P180 abrasive paper

Material	ΔRF (%)	ΔTF (%)	ΔAF (%)
PET	+2695.62	−22.45	+59.82
PP	+18.01	−4.96	−4.95
PTFE	+5.35	−12.75	−4.95
PA	+11.40	−7.09	−4.80

while highest of transmitted share, ranging from ~90.3% for the AS sample to 70.0% following P180 treatment (please refer to Fig. 11). Comparing the P800 treatment of PET with that of PP (please refer to Fig. 12), for the latter the reflected energy fraction assumes almost a double value, i.e., ~18.0% against 10.1%, while the absorbed share is about five times greater, i.e., ~38.3% against 7.5%. PTFE has the lowest percentage of transmitted percentage, ranging from ~19.6% for the AS sample to ~16.7% following P400 treatment, and the highest percentage of reflected share, ranging from ~62.9% for the AS sample to ~69.2% following P400 treatment (please refer to Fig. 13), while PA has the highest percentage of absorbed energy fraction, ranging from ~35.1–40.9% (please refer to Fig. 14) followed by PP, ranging from ~33.2% to ~38.3%, as schematically illustrated in Fig. 12 and in Table 5. Table 6 summarizes the overall percentage variations of the reflected (RF), transmitted (TF) and absorbed (AF) energy fractions by polymers following surface treatments with P180 abrasive paper. In agreement with the above (please refer to Figures from 11 to 14), PET is the material that undergoes the largest percentage increase in RF, i.e., ~2695.6%, and the largest percentage decrease in TF, i.e., ~22.5%; while PTFE is the material that undergoes the smallest RF increase after corrugation with P180 abrasive paper, i.e., ~5.3%. Intermediate is the behaviour of PP and PA, with an increase in RF of ~18.0% for PP and 11.4% for PA, respectively.

In laser transmission welding, the importance of the phenomenon of absorption and transmission of light radiation through the thickness of the polymer up to the point of joint with the metal has been already highlighted in the literature. The polymers chosen for LTW should ensure laser transmission and absorption (when the material is adopted to absorb the radiation) [18]. The laser light absorbed into the material propagates and gradually transfers its energy in the form of heat [11, 36]. The heat produced in the material can eventually lead to material modifications or

melting of the material needed for laser welding [37]. Only in the latter case it is possible to obtain the formation of the joint. In this regard, the trends in the histograms (Figs. from 11, 12, 13, and 14) and Tables 5 and 6 reveal detrimental trends in the energy shares for the abraded materials. In fact, a general decrease in the transmitted and absorbed fractions and an adverse increase in the reflected shares is obtained, for all polymers. The most notable exception is the increase in AF in the case of PET, i.e., from ~9.2% to ~14.7%, ollowing P80 treatment; in any case the variation is significantly lower than the changes in TF and RF (please refer to Fig. 11). PTFE has the lowest values of the transmitted energy percentage and the highest values of the reflected fractions compared to the other materials. Compared to PET, the percentage of the transmitted radiation is even more drastically reduced (by treating with P800 it drops to 82.4% and ~17.2% or PET and TFE, respectively) in favour of the reflected share.

Since laser application in welding relies on the thermo-optical relationship between the laser beam and the target material, the last one should not be highly reflective, as the portion of the laser beam that is not reflected enters the material [14, 38]. Figure 15 shows the diagram of the surface reflected fraction, for the different polymers, as a function of the roughness parameter Ra, in single-plate test configuration. The short trend of the profile recorded for PTFE follows the less significant variation of the roughness parameters Ra and Rz undergone for this material following the treatment. The presence of surface roughness causes a decrease in the transmitted share which is more significant in the case of PET (i.e., ΔTF average of ~22.5%), whch contributes to the reflected energy percentage; the reflected fraction on the surface passes from ~0.5% to ~5.3% whenthe roughness Ra passes from ~0.04 to about 2.33 µm (with abrasive grit P180).

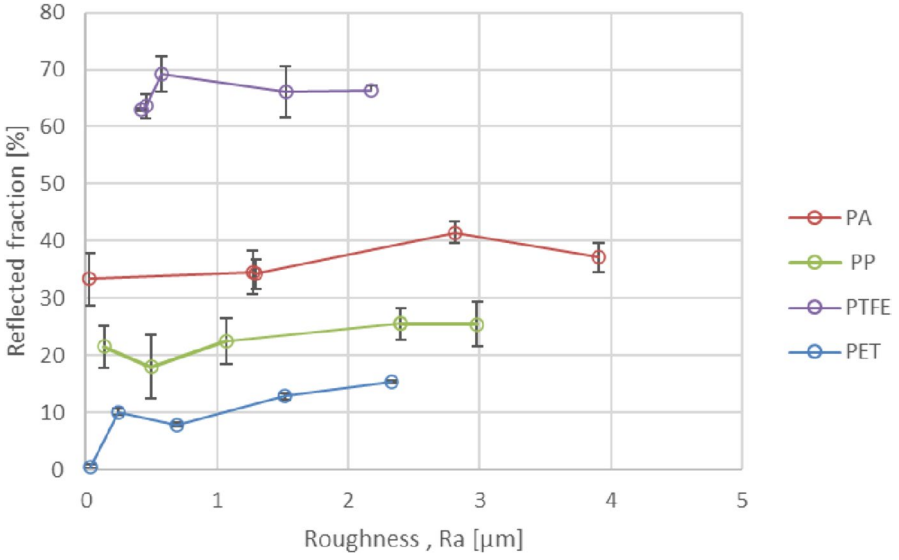

Fig. 15 Reflected energy fraction on the surface as a function of surface roughness for the different polymers

As a result, an incoming laser beam on a smoother surface should promote the transmission of the radiation towards the joining point and therefore be more convenient in laser joining operations. On the other hand, it can be assumed that by shifting the roughness of the polymer from the entry surface to the exit surface of the laser beam, the total internal reflection might increase, favouring the joint at the interface point with the metal.

Lye et al. [39] analyzed the surface roughness effect of sapphire samples on light transmission. This investigation demonstrated that the orientation of the rough surface with respect to a laser beam source is a key parameter on total internal reflection, and thus nonlinear absorption. This phenomenon was significant and effective in trapping the laser light energy within the sample enhancing the nonlinear absorption required for laser machining. Therefore, the orientation of the rough or smooth surface towards or away from the laser source (i.e., if the laser is an incident or exit beam) is a critical parameter of the processing outcomes.

We didn't find any others investigations on the existence of total internal reflection caused by surface roughness, and its significance on laser beam energy absorption in laser radiation-material interaction. Based on the experimental results, we hypothesise that it is potentially possible to exploit the same mechanism of total internal reflection by applying it to the polymer. In fact, the increase in the reflected energy share in this case would occur towards the inside of the material, thus providing an increase in energy at the joint point.

Conclusions

LTW has now become a well-established laser-based polymer welding technique that offers several process advantages over conventional polymer welding techniques. In LTW the laser beam passes through the thermoplastic joining partner and is absorbed at the boundary layer between metal and plastic. This leads to a high thermal load of the polymer at the contact area and requires a transmittance of the plastic material within laser radiation wavelength. A fundamental role in LTW is therefore played by the study of the fractions of the reflected, absorbed, and transmitted radiations by the polymeric surface.

In this research, samples of semi-crystalline polymers of PET, PP, PTFE, PA were subjected to surface treatments with different abrasive papers (from P180 to P180) to study the influence of roughness on radiation energy shares. The most important results of the research can be summarized as follows:

- PET, with the lowest values of the roughness parameters both before and after the treatment, appears to be the most influenced by the surface treatment, recording the greatest increase in the Rz parameter (about 37 times). PTFE and PA are the least affected materials, with an increase of Rz of about 5 and 6 times respectively;
- A simple and effective method to experimentally calculate the Beer-Lambert law for the polymeric plates (with various degrees of surface roughness) exposed at a laser beam wavelength of 975 nm was set up and validated. The experimental setup

adopted allowed to directly measure the transmitted power as a function of the sample thickness. The reflected energy fractions were obtained from the experimental equations and the absorbed ones from the energy balance;

- A good correlation (i.e., R^2 values of ~1) was found between the exponential law and the experimental measures and a decrease in the power transmitted by the polymers as the degree of surface roughness increased, in particular for PET. For PTFE, the transmitted share undergoes a more contained decrease, reflecting the minor influence of the surface morphology (i.e., of the roughness parameters) from the treatment applied;
- The general decrease in the transmitted and absorbed energy fractions and an unfavourable increase in the reflected shares represent a detrimental effect in LTW applications, since it is the portion of the laser beam that enters the material that allows the creation of the hybrid joint. This phenomenon was mainly observed for PET, with an increase in the RF of the material from ~0.5% to ~15.3%, when the roughness Ra passes from ~0.04 to about 2.33 μm, following P180 treatment.

Based on experimental results, it is finally assumed that the transfer of roughness from the incoming surface to the outgoing surface of the laser beam might provide the opposite result: an increase in total internal reflection, able to help the joint at the interface point with the metal. This research, therefore, proposes as a future development the characterization of the roughening effect on the polymer surface away from the laser source, an empirical study that in the literature to date has only been successfully applied and experimentally validated to a mineral sample.

Author Contributions Silvio Genna: Conceptualization, Formal analysis, Data curation, Investigation, Methodology, Resources, Supervision, Project administration, Funding acquisition, Writing - Review & Editing.Patrizia Moretti: Data curation, Formal analysis, Investigation, Methodology, Software, Writing - Original Draft, Writing - Review & Editing; Claudio Leone: Conceptualization, Data curation, Formal analysis, Investigation, Methodology, Software. Simone Venettacci: Investigation, Resources, Project administration, Funding acquisition, Writing - Original Draft, Writing - Review & Editing.

Funding Open access funding provided by Università degli Studi di Roma Tor Vergata within the CRUI-CARE Agreement. This study has been funded through the Programma Operativo Regionale - POR FESR Lazio 2014–2020, Call "Gruppi di Ricerca 2020", Project A0375–2020 – 36716 "Laser joIning fOr New hybrid Structures - LIONS" - CUP: E85F21000820005.

Data Availability All the data will be available on request.

Declarations

Ethical Approval Not applicable.

Competing Interests The authors declare no competing interests.

References

1. Mistry, K.: Plastics welding technology for industry. Assem. Autom. **17**, 196–200 (1997). https://doi.org/10.1108/01445159710172210
2. Haque, M.S., Moeed, K., Zaka, M.Z.: Laser welding of thermoplastics – A review. Mater. Today Proc. **64**, 1479–1485 (2022). https://doi.org/10.1016/J.MATPR.2022.04.900
3. Jones, I.: Laser welding for plastic components. Assem. Autom. **22**, 129–135 (2002). https://doi.org/10.1108/01445150210697429
4. Charlson, P.M., Schwieters, C.R., Souk, J.H.: Laser joining of thermoplastic and thermosetting materials. US Patent. **4414166** (1983)
5. Potente, H., Korte, J., Becker, F.: Laser Transmission Welding of Thermoplastics Analysis of the Heating Phase. J. Reinf. Plast. Compos. **18** (1999)
6. Coelho, J.P., Abreu, M.A., Pires, M.C.: High-speed laser welding of plastic films. Opt. Lasers Eng. **34**, 385–395 (2000). https://doi.org/10.1016/S0143-8166(00)00071-3
7. Duley, W.W., Mueller, R.E.: CO2 laser welding of polymers. Polym. Eng. Sci. **9**, 582–585 (1992)
8. Huang, Y., Gao, X., Zhang, Y., Ma, B.: Laser joining technology of polymer-metal hybrid structures - a review. J. Manuf. Process. **79**, 934–961 (2022). https://doi.org/10.1016/j.jmapro.2022.05.026
9. Xu, X.F., Bates, P.J., Zak, G.: Effect of glass fiber and crystallinity on light transmission during laser transmission welding of thermoplastics. Opt. Laser Technol. **69**, 133–139 (2015). https://doi.org/10.1016/J.OPTLASTEC.2014.12.025
10. Berger, S., Oefele, F., Schmidt, M.: Laser transmission welding of carbon fiber reinforced thermoplastic using filler material—A fundamental study. J. Laser Appl. **27**, S29009 (2015). https://doi.org/10.2351/1.4906391
11. Kagan, V.A., Bray, R.G., Kuhn, W.P.: Laser transmission welding of semi-crystalline thermoplastics-part I: Optical characterization of nylon based plastics. J. Reinf. Plast. Compos. **21**, 1101–1122 (2002). https://doi.org/10.1177/073168402128987699
12. Jaeschke, P., Wippo, V., Suttmann, O., Overmeyer, L.: Advanced laser welding of high-performance thermoplastic composites. J. Laser Appl. **27**, S29004 (2015). https://doi.org/10.2351/1.4906379
13. Messler, R.W.: Trends in key joining technologies for the twenty-first century. Assem. Autom. **20**, 118–128 (2006). https://doi.org/10.1108/01445150010321733
14. Acherjee, B.: Laser transmission welding of polymers – A review on process fundamentals, material attributes, weldability, and welding techniques. J. Manuf. Process **60**, 227–246 (2020). https://doi.org/10.1016/j.jmapro.2020.10.017
15. Schricker, K., Stambke, M., Bergmann, J.P.: Adjustment and Impact of the Thermoplastic Microstructure of the Melting Layer in Laser-based Joining of Polymers to Metals (2015)
16. Arai, S., Kawahito, Y., Katayama, S.: Effect of surface modification on laser direct joining of cyclic olefin polymer and stainless steel. Mater. Des. **59**, 448–453 (2014). https://doi.org/10.1016/J.MATDES.2014.03.018
17. Acherjee, B.: State-of-art review of laser irradiation strategies applied to laser transmission welding of polymers. Opt. Laser Technol. **137**, 106737 (2021). https://doi.org/10.1016/J.OPTLASTEC.2020.106737
18. Gonçalves, L.F.F.F., Duarte, F.M., Martins, C.I., Paiva, M.C.: Laser welding of thermoplastics: An overview on lasers, materials, processes and quality. Infrared Phys. Technol. **119**, 103931 (2021). https://doi.org/10.1016/J.INFRARED.2021.103931
19. Bergmann, C.P.: Topics in Mining, Metallurgy and Materials Engineering Series Editor, n.d. http://www.springer.com/series/11054
20. Gisario, A., Aversa, C., Barletta, M., Natali, S., Veniali, F.: Laser joining of aluminum film coated with vinylic resin and plastic/bioplastic films for applications in food packaging. Opt. Laser Technol. **142**, 107237 (2021). https://doi.org/10.1016/J.OPTLASTEC.2021.107237

21. Brown, N., Kerr, D., Parkin, R.M., Jackson, M.R., Shi, F.: Non-contact laser sealing of thin polyester food packaging films. Opt. Lasers Eng. **50**, 1466–1473 (2012). https://doi.org/10.1016/J.OPTLASENG.2012.04.001
22. Kagan, V.A.: Innovations in laser welding of thermoplastics: This advanced technology is ready to be commercialized (2018)
23. Kagan, V., Bray, R.G.: Advantages and limitations of laser welding technology for semi-crystalline reinforced plastics. Laser Inst. Am. 1218–1227 (2018). https://doi.org/10.2351/1.5059784
24. Chen, M., Zak, G., Bates, P.J.: Effect of carbon black on light transmission in laser welding of thermoplastics. J. Mater. Process Technol. **211**, 43–47 (2011). https://doi.org/10.1016/j.jmatprotec.2010.08.017
25. Niu, C., Zhu, T., Lv, Y.: Influence of surface morphology on absorptivity of light-absorbing materials. Int. J. Photoenergy **2019**, 1 (2019). https://doi.org/10.1155/2019/1476217
26. Su, F.-G., Liang, J.-Q., Liang, Z.-Z., Zhu, W.-B.: Study on the surface morphology and absorptivity of light-absorbing materials. Acta Phys. Sin. **60** (2011).
27. Chen, J., Zhang, Q.L., Yao, J.H., Fu, J.B.: Influence of surface roughness on laser absorptivity. Laser Technol. **32**, 624 (2008)
28. Wang, C.Y., Bates, P.J., Zak, G.: Optical properties characterization of thermoplastics used in laser transmission welding: Scattering and absorbance. Adv. Mat. Res. 3836–3841 (2010). https://doi.org/10.4028/www.scientific.net/AMR.97-101.3836
29. van de Ven, J.D.: Simultaneous measurement of laser reflection and transmission of poly(vinyl chloride). Opt. Eng. **45**, 094301 (2006). https://doi.org/10.1117/1.2353269
30. Grewell, D., Rooney, P., Kagan, V.A.: Relationship between optical properties and optimized processing parameters for through-transmission laser welding of thermoplastics. J. Reinf. Plast. Compos. **23**, 239–247 (2004). https://doi.org/10.1177/0731684404030732
31. Genna, S., Leone, C., Tagliaferri, V.: Characterization of laser beam transmission through a high density polyethylene (HDPE) plate. Opt. Laser Technol. **88**, 61–67 (2017). https://doi.org/10.1016/J.OPTLASTEC.2016.08.010
32. Lopatková, M., Bárta, J., Marônek, M., Šugra, F., Kritikos, M., Samardžić, I., Marić, D.: The influence of surface roughness on laser beam welding of aluminium alloys. Tehnicki Vjesn. **28**, 934–938 (2021). https://doi.org/10.17559/TV-20201102100726
33. Di Siena, M., Genna, S., Moretti, P., Ponticelli, G.S., Venettacci, S., Russo, P.: Study of the laser-material interaction for innovative hybrid structures: Thermo-mechanical characterization of polyethylene-based polymers. Polym. Test. **120**,(2023). https://doi.org/10.1016/J.POLYMERTESTING.2023.107947
34. Gijsman, P., Meijers, G., Vitarelli, G.: Comparison of the UV-degradation chemistry of polypropylene, polyethylene, polyamide 6 and polybutylene terephthalate. Polym. Degrad. Stab. **65**, 433–441 (1999). https://doi.org/10.1016/S0141-3910(99)00033-6
35. Azhikannickal, E., Bates, P.J., Zak, G.: Use of thermal imaging to characterize laser light reflection from thermoplastics as a function of thickness, laser incidence angle and surface roughness. Opt. Laser Technol. **44**, 1491–1496 (2012). https://doi.org/10.1016/j.optlastec.2011.12.013
36. Kumar, D., Acherjee, B., Kuar, A.S.: Laser transmission welding: A Novel Technology to join polymers. Encycl. Mater.: Plast. Polym. **1–4**, 338–352 (2022). https://doi.org/10.1016/B978-0-12-820352-1.00126-7
37. Anwer, G., Acherjee, B.: Laser polymer welding process: Fundamentals and advancements. Mater. Today Proc. **61**, 34–42 (2022). https://doi.org/10.1016/J.MATPR.2022.03.307
38. Acherjee, B., Kuar, A.S., Mitra, S., Misra, D.: Application of grey-based Taguchi method for simultaneous optimization of multiple quality characteristics in laser transmission welding process of thermoplastics. Int. J. Adv. Manuf. Technol. **56**, 995–1006 (2011). https://doi.org/10.1007/s00170-011-3224-7
39. Lye, C.S.M., Wang, Z.K., Lam, Y.C.: Mechanism and effects of surface morphology on absorption characteristics in ultrashort pulse laser processing of sapphire. Appl. Surf. Sci. **542** (2021). https://doi.org/10.1016/j.apsusc.2020.148734

Authors and Affiliations

Silvio Genna[1] · Claudio Leone[2] · Patrizia Moretti[1] · Simone Venettacci[3]

✉ Silvio Genna
silvio.genna@uniroma2.it

[1] Department of Enterprise Engineering, University of Rome Tor Vergata, Via del Politecnico 1, Rome 00133, Italy

[2] Department of Engineering, University of Campania "Luigi Vanvitelli", Via Roma 9, Aversa 81031, Italy

[3] Department of Engineering, University of Rome Niccolò Cusano, Via Don Carlo Gnocchi 3, Rome 00166, Italy